LAWRENCE
LIVERMORE
NATIONAL
LABORATORY

LLNL-JRNL-644784

High-adiabat high-foot, low-mix cryogenic DT layered capsule implosion experiments on the National Ignition Facility

H. S. Park, O. A. Hurricane, D. A. Callahan, D. T. Casey, E. L. Dewald, T. R. Dittrich, T. Doppner, D. E. Hinkel, L. F. Berzak Hopkins, S. Le Pape, T. Ma, P. K. Patel, B. A. Remington, H. F. Robey, J. Salmonson, J. L. Kline

October 11, 2013

Physical Review Letters

Disclaimer

High-adiabat high-foot, low-mix cryogenic DT layered capsule implosion experiments on the National Ignition Facility

H.-S. Park*, O. A. Hurricane, D. A. Callahan, D. T. Casey, E. L. Dewald, T. R. Dittrich, T. Doeppner, D. E. Hinkel, L. F. Berzak Hopkins, S. Le Pape, T. Ma, P. K. Patel, B. A. Remington, H. F. Robey, J. D. Salmonson

Lawrence Livermore National Laboratory

J. L. Kline

Los Alamos National Laboratory

This letter reports on an experimental campaign of cryogenic layered deuterium-tritium (DT) indirectly driven implosions using a high-adiabat drive on National Ignition Facility. The high-adiabat implosion platform is designed to give a robust implosion that is resistant to ablation-front Rayleigh-Taylor instability induced mix of ablator material into the DT hot-spot. In this 5 shot campaign on NIF, the observed hot spot mix was low and observed neutron yield over simulated was typically 50% or higher. The highest performing shot of this campaign used 1.7 MJ laser energy at 350 TW peak power and peak radiation temperature of ~300 eV (?). The experimentally observed results were primary DT neutron yield of 2.4 x 10^{15}, fuel ρR of 0.84 g/cm^2, and T_{ion} of 4.2 keV, corresponding to 8 kJ of fusion yield, with ~1/3 coming from alpha-particle self-heating.

DOI:

PACS number: 52.57.Fg, 52.70.La, 52.70.Nc

* park1@llnl.gov; hurricane1@llnl.gov

The goal of ignition experiments on the National Ignition Facility (NIF) [1] is to achieve fusion ignition by compressing deuterium-tritium (DT) fuel to ~1000 g/cc and heating a central hot-spot to T_{ion}~10 keV. High levels of DT fuel convergence (convergence ratio's, CR~35-45), are achieved by keeping the fuel adiabat (α) as low as possible. Previous implosions used a weak first shock, driven by a holhraum radiation temperature of ~60 eV – a "low-foot" – followed by 3 other shock the timing and level of which are designed to achieve high implosion speeds while minimizing adiabat α and maximizing DT fuel areal density. Very high levels of compression, hence high values of convergence ration (CR), are needed to reduce the ignition energy requirements, which scale as CR^{-6}, and this was the primary rational for keeping the fuel adiabat in the implosion low. Prior to the high-foot campaign, the best performing implosions produced maximum neutron yield of 7.5×10^{14} neutrons with down-scatter ratios (*DSR*, a measure of fuel areal density, ρR) of 6.4 g/cm^2. These implosions experimentally measured yield-over-clean simulations (*YOC*) at the level of 5-25% without including contributions from the alpha-particle self-heating in the simulations [2]. One component of the degraded level of performance was thought to be coming from Raleigh-Taylor instability of the ablation front [3] causing the implosion to be more susceptible to mix of the ablator material (CH) into the DT fuel.

Alpha-particle self-heating is a necessary condition for ignition as it is the key mechanism that deposits fusion energy back into the fusion fuel, creating the necessary boot-strapping of temperature and the creation of yet more alpha-particles (and neutrons which generally do not participate in self-heating and just leave the yield producing region). Alpha particles will self-heat, in an inertial confinement fusion implosion, if trapped in the hot spot by sufficiently high ρR in the DT and if the T_{ion} is sufficiently high that the fusion reaction rate is

rapid as compared to the hot-spot disassembly time. Roughly, ignition will occur when $\rho R_{\text{hot-spot}}$ ~ 0.3 g/cm^2 and T_{ion} ~ 10 keV and propagation to high-gain will occur when $\rho R_{\text{fuel}} > 1$ g/cm^2.

A recently developed metric for gauging an implosions distance from ignition (defined as 1 MJ yield) is the ignition threshold factor (ITFX) [4] that is unity at ignition. ITFX is formulated to be:

$$ITFX = \frac{{Y_n}^{13-15MeV}}{4\times10^{15}} \cdot \left(\frac{DSR^{10-12MeV}}{0.067}\right)^{2.1} \quad (1)$$

where ${Y_n}^{13-15MeV}$ is the neutron yield observed with energies between 13 and 15 MeV energy range and $DSR^{10-12MeV}$ is the down-scattered ratio of the number of neutrons scattered into the 10 to 12 Mev energy range to Y_n. Another metric that measures nearness to ignition of an implosion is the Generalized Lawson Criterion (GLC) [5]. GLC is derived from the definition where the fusion energy production rate is equal to the plasma loss rate and is closely related to the criteria used in magnetic fusion contexts.

$$\chi = \left[\frac{\rho R}{1.5}\left(\frac{T_{ion}}{3.8}\right)^{2.2}\right]^{0.8} \quad (2)$$

The GLC is closely related to alpha-deposition in the hot-spot and to the energy done on the hot-spot by *PdV* work. Below, both metrics are applied to understand the high-foot implosion campaign shot performance.

Hydrodynamic instabilities such as the Rayleigh-Taylor (RT) and Richtmyer-Meshkov (RM) instabilities can cause capsule surface and interface imperfections to grow. If severe enough, this can cause ablator material to mix into the core and radiatively cool the hot spot, decreasing the hot spot temperature and nuclear yield. The high-foot pulse-shape is designed to

increase the ablation velocity and density gradient scale length at the ablation front, both of which reduce the ablation front RT growth. A consequence of this approach to decreasing the RT growth and hot spot mix, however, is to also decrease the expected peak compression and fuel areal density.

The required radiation drive for this high-foot design was reverse engineered into the pulse shape shown in Fig 1. The radiation drive vs. time and details of the theoretical design are described in a companion letter [6]. The pulse uses ~40 TW in the picket (the beginning of the pulse), then ~3 TW in the trough which combined makes up the drive foot, and ~40 TW to launch the second shock. In the high-foot experimental campaign describe here, the peak laser power was varied between 350 TW to 430 TW and the total laser energy was varied from 1.3 MJ to 1.7 MJ. The laser delivered the required power and energy at every part of the pulse shape history to within 5% of request.

In order to control the cross-beam transfer, we use 2-color and 3-color laser wavelength corrections [7]. For the high-foot shots, we used an 8.5 Å wavelength difference between the 23 degree cone to the outer cones (45 degree and 50 degree) beams and 7.3Å wavelength difference between the 30 degree beams to the outer cones. The measured backscatter indicates that the laser energy coupling efficiency is ~88% on average, as compared to the low-foot shots that average ~85%. The slightly improved coupling efficiency is mostly due to the higher hohlraum ^{4}He gas-fill density (1.6 mg/cc) associated with the high-foot pulse-shape, that is more effective at restricting the blow-off of gold plasma from the hohlraum wall as the radiation temperature increases.

A nominal dimension hohlraum [5.75 mm diameter, 3.1 mm diameter laser entrance hole (LEH) and is 9.4 mm long] was used in most of the high-foot campaign. The capsule dimensions

and silicon dopant levels and profiles used in this 5-shot high-foot campaign have been the same as those used for the low-foot campaign [8]: the inner capsule radius is 935±8 μm and the ablator thickness is 195±3 μm at cryogenic temperatures. The ablators consisted of 5 layers of graded density CH plastic doped with varying silicon atomic fractions in order to tailor the density profile in the ablator such that the Atwood number is favorable during the acceleration and deceleration phases of the implosion.

A full suite of nuclear and x-ray diagnostics are employed to measure the performance of the cryogenic DT implosions . Near the time of implosion stagnation, the hot-spot shapes are measured by time resolving framing cameras as well as with time integrating image plates from both the equator side (DIM90-78) and the polar view (DIM00-00). The neutron shapes are measured by the neutron imaging system (NIS) which captures spatial information on direct (13-17 MeV) neutrons and down-scatted neutrons (6-12 MeV). The DT fusion yield is measured by many instruments including neutron time-of-flight detectors (NToF) and nuclear activation detectors (NAD's) that are distributed around the NIF target chamber. The official reported yield values are the weighted average of all the measurements. The T_{ion} is measured by the width of the NToF signals of both DT and DD neutron reactions, accounting their thermal kinematics [9].

A total of 5 high-foot shots were performed as of Aug 13, 2013. One of these shots (N130802) used different length (10.1 mm) hohlraum and another (N130710) had a far out-of-tolerance DT ice layer with a ~5 μm m=1 mode offset -- these two shots are not discussed in this paper, but will be in a future paper. The summary of experimental performance of the remaining three key high-foot DT layered shots is given Table I. In the table the coasting time (the time between when the laser is turned off and bang time) is noted. We listed only nuclear bang-time, because the x-ray bang-time is about the same as the nuclear bang-time to within the experimental

error. The x-ray burn-width follows the same trend as the nuclear burn widths, as well. The mix mass number is inferred from the x-ray yields above the clean Bremsstrahlung ablator emission [10]. For the high-foot shots in this 5-shot campaign, the inferred mix mass has been <200 ng, indicating very low mix, confirming one of the key goals of the campaign. Once the shape is determined, the implosion stagnation pressure can be calculated using the measured *DSR*, T_{ion}, and constructed volume [11]. The velocities are not directly measured; instead they were scaled from the 1D ConA [12, 13] measurements that used the same high-foot 1st and 2nd shock pulses but used a lower peak power. The last column of Table 1 contains the results from the 2D hohlraum simulation for the performance parameters for the N130812 shot. From this simulation, the YOC for N130812 is close to 70%. However, T_{ion} and DSR are lower than the experimental measurements.

As an example, the hotspot shape measured by the x-ray cameras [Ref] and neutron imaging systems [Ref] for N130812 are shown in Fig 2. The equatorial shape is oblated with double lobed features and the polar view shows the toroidal shape. The pre/post shot simulations (bottom row) show similar shape. We attribute the asymmetry comes from the hohlraum drive [Add more, Denise]. We have reconstructed the shape into a toroidal hot spot shape using the measured P0 size. While the shape is not spherical, the surface to volume ratio of our hot-spot and the pressures are not so much different from being round. The hot-spot and downscattered neutron images from all the highfoot series are studied in terms of their effect on the implosion performance. N130501 had the roundest hot-spot shot of any DT shot in the high-foot series as indicated by the equatorial $[r_p(\theta) = P0(1 + \frac{P2}{P0}P_2(\cos(\theta)) + \cdots)]$ and polar $[r_m(\theta) = M0(1 + \frac{M2}{M0}P_2(\cos(\theta)) + \cdots)]$ Legendre mode hot spot perimeter shape measurements are noted in Table I. The subsequent shot, N130710, used more laser power to obtain higher performance, but it was

observed that the shape of the imploded hot-spot became more distorted, becoming more oblate in the equatorial (P) view and generating an obvious torus shape in the polar (M) view. For shot N130812, the laser power was reduced to the same level as N130501, but the energy was increased in order to reduce "coasting" in the implosion. N130812 achieved very high performance and the hot-spot shape was improved over N130710, but still showed evidence of a compact toroidal hot-spot.

The equatorial shape is oblate, but not as much as in N130710, and the polar view shows the clear toroidal shape with some evidence of m=4 mode structure. The post-shot 2D axisymmetric simulations (bottom row) show similar shape. The toroidal shape is likely a consequence of a known P4 mode [Legendre $P_4(\cos\theta)$ mode] that is imposed on the ablator due to the beam pointing on the hohlraum wall [15]– an effect that has been previously recognized as an issue in the nominal length hohlraum. Presently, it is believed that the oblate shape of the higher power, N130710, shot and the higher energy, N130812, shot is due to restricted inner beam laser propagation at late time that slightly cools the radiation drive at the waist of the implosion as compared to the poles. Striking is the fact that the high-foot shots have high yields along with high Yield-Over-Clean (YOC). Here we define the YOC to be the experimental DT yield in 13-15 MeV range over the 1D simulation DT yield with alpha particle energy deposition physics turned on. While the hot-spot shape is not spherical in the experiments, the surface to volume ratio, volume, and therefore pressure of the hot-spot are not greatly different from being round. This is the reason why 1D models still compare well with the data on yields. On N130812 the measured T_{ion} of 4.2 keV (from DT NToF) is higher than the simulations by several hundred eV (this particular datum is curious and not fully understood at this time as the T_{ion} from the DD NToF is ~3.5 keV which is more consistent with the models). The *DSR* on N130812 was also higher than

simulation expectations. On shots N130501 and N130710 the measured and simulated T_{ion}'s agree as do the *DSR* values.

The first shot of the series, N130501, formed the baseline for the high-foot series and it outperformed previous NIF shots (Fig. 3) in total yield, but had by design lower fuel ρR (Fig. 4). The fuel rR is derived by: $\rho R\left(\frac{g}{cm}^2\right) = 21\times DSR_{13-15MeV}$. N130812 produced more neutrons than the pre-shot prediction of 1D simulation without alpha particle energy deposition physics turned on. This indicates that alpha-particle self-heating augmented the total DT neutron yield in the experiment. At the moment, there is no direct way to experimentally measure or distinguish the difference between how much of the measured yield was from the alpha-particle self-heating contribution versus the compressional yield, without performing an identical shot with a diluted (tritium rich-deuterium poor) DT ice layer. The estimated amount of alpha-particle self-heating comes from the results from the 1D and 2D simulations with alpha-particle heat deposition turned on and off. Fig 3 shows yield performance of the all cryogenic DT shots on NIF over the last 3 years.

In Fig. 3 the component of the yield coming from alpha-particle self-heating is shown in red and the energy reflecting that of fuel compression output as yield is shown in blue. In shot N130812, 6.4 kJ of energy was released as neutrons with 1.6 kJ of alpha-particle energy reabsorbed. The total hot-spot energy was 3.4 kJ. Total energy delivered into the fuel was 10.3 kJ. The hot-spot density in N130812 was ~ 25 g/cc. Approximately, a 50% yield amplification from self-heating is inferred.

Fig. 4 shows the performance of the high-foot campaign DT shots (green) and that of previous low-foot implosions (grey) plotted against yield and fuel ρ*R*. In general, the figure illustrates the trade-off of compression in exchange for higher performance. In fig. 4, contours of

the ratio of yield with and without alpha-particle energy deposition ($Y_{\alpha}/Y_{no\text{-}\alpha}$) are noted. Error bars on yield are too small to show up on the plot, while the error bars on fuel ρR are clear.

Fig. 5 (a) shows the experimentally obtained yield performance of cryogenic DT shots on NIF plotted against the yield expected from 1D simulation. As can be observed, generally the high-foot shots exhibit higher YOC and higher absolute performance. A major component of the lower performance, as compared to simulation, of the low-foot implosions as shown in Fig. 5 (a) was thought the be driven, at least in part by significant ablative Rayleigh-Taylor instability and mix -- the results presented in this paper appear to support the assertion. Fig. 5 (b) is the DT yield vs the Generalized Lawson Criterion (GLC) as defined in eq (2). GLC's for the series of shots N130501, N130710, and N130812 are χ=0.21, 0.26, and 0.42 respectively. GLC of χ=0.54 is required for a yield doubling due to alpha-particle self-heating. It clearly shows that N130812 achieved a very high GLC further supporting high YOC for this event.

These high-adiabat / high-foot implosion experiments show remarkably high performance despite their somewhat low-mode asymmetric shape. We attribute this higher performance to reduction of the ablator mi, generated by the Raleigh-Taylor instability, into the hot-spot. This is further confirmed by experimental measurements, highdro growth radiography campaign, of growth of the ablator layer comparing both high-foot and low-foot pulses [HGR Ref]. The low mode hot-spot shapes, parameterized by P2/P0, M4, show somewhat asymmetric implosion. Despite these asymmetries, their higher nuclear performance indicates that the low-mode implosion shape is not a dominating factor at this early stage of compression but the high-mode mix plays a more important role. We caution that the HGR campaign measured the RT growth only in the mid modes of ~60; the higher mode RT growth factor measurements are more challenging the experimental technique are being refined to obtain higher resolution experimental

data. However, this HGR results and the simulation strongly supports that the high-foot, high-adiabat suppresses the ablator front RT instabilities providing a new platform to control the high-mode mix at early stage of the implosion process.

In conclusion, the performance of indirectly-driven DT layered implosions utilizing the high-adiabat / high-foot pulse shape have been presented in the letter. The results of the five shot high-foot series appear to support the idea that ablation front Rayleigh-Taylor instability and mix was a major factor in the degraded performance observed under with NIC implosions. Additional, the high-foot implosions have out-performed the NIC implosions in yield and with shot N130812 ignition metric. Future plans for the series involve accessing higher implosion speeds with dual paths of addressing hohlraum physics, thinner CH ablators, and alternate ablator materials.

We'd like to thank the entire NIF operations team. This work was performed under the auspices of the U.S. Department of Energy by Lawrence Livermore National Laboratory under Contract No. DE-AC52-07NA27344.

Figure Captions:

Table 1. Summary of experimentally measured performance parameters from the three high-foot shots.

Fig. 1. Laser power vs. time are shown for a representative low-foot (NIC) pulse-shape (black) and high-foot pulse-shapes (N130710 in blue and N130812 in red). Salient features are a higher picket power and a shorter pulse in the high-foot cases as well as the removal of the second laser impulse (seen in the low-foot case near 13 ns) which, from the capsule perspective, drops a shock.

Fig. 2. From left-to-right, the figure shows images of emission intensity in equatorial view x-rays, polar view x-rays, equatorial view direct (13-15 MeV) neutrons, and equatorial view in-direct (6-12 MeV) neutrons. The color-scale reflects emission intensity (red is high intensity, blue is low). The upper row shows the images from experiment N130812. The lower row shows results from post-shot 2D Hydra simulations.

Fig. 3. Yields from NIF shots are plotted versus date (year-month-day format, YYMMDD). Yield from fuel compression is shown in blue and yield from alpha-particle self-heating is shown in red.

Fig. 4. The plot shows a scatter plot in total DT neutron yield and fuel ρR (g/cc) of NIF shot performance for the low-foot (NIC) series (grey dots) and high-foot series (green boxes). Contours of alpha-heating multiplication are shown as the blue curves. The key shots that are the discussed in this paper are labeled by shot number: N130501, N130710, and N130812.

Fig. 5. Plotted is the total experimentally determined yield versus the yield predicted by 2D simulation. The diagonal dashed lines show contours of YOC. The green squares are the high-foot series of shots and the blue series of dots are for the low-foot (NIC) campaign.

[1] J. D. Lindl and E. I. Moses, Phys. Plasmas, **18**, 050901 (2011).

[2] M.J. Edwards, *et al.* Phys. Plasmas, **20**, 070501 (2013).

[3] V. Gonchorov and O. A. Hurricane, "Panel 3 Report: Implosion Hydrodynamics", LLNL Report, LLNL-TR-562104, (2012). *Op cit.* "Science of Fusion Ignition on NIF Workshop May 22-24, 2012," LLNL Report, LLNL-TR-570412 (2012).

[4] B. K. Spears *et al.,* Phys. Plasmas, **19**, 056316 (2012).

[5] C. D. Zhou and R. Bett, Phys. Plasmas, **16**, 079905 (2009).

[6] T. R. Dittrich, O.A. Hurricane, D.A. Callahan, E.L. Dewald, T. Doeppner, D.E. Hinkel, L.F. Berzak Hopkins, S. Le Pape, T. Ma, J.L. Milovich, P.K. Patel, H.-S. Park, B.A. Remington, J.D. Salmonson, Phys. Rev. Lett., submitted (2013).

[7] P. Michel, *et al*., Phys. Rev. Lett. **102**,025004 (2009).

[8] S.W. Haan, *et al*., Phys. Plasmas, **18**, 051001, (2011).

[9] NTOF paper or diag paper

[10] T. Ma, *et al*., Phys. Rev. Lett., **111**, 085004 (2013).

[11] P. T. Springer and C. Cerjan, (2011).

[12] D. Hicks, 1D conA paper

[13] E. Dewald, 1D conA paper

[14] O. Hurricane *et al*., in preparation, Nature (2013)

[15] O.L. Landen, *et al*., Phys. Plasmas, **18**, 051002 (2011).

	N130501	N130710	N130812	Simulation prediction for N130812
Laser Energy (MJ)	1.292	1.484	1.693	input
Peak Power (TW)	353.7	433.9	354.9	input
Coasting Time (ns)	2.1	1.8	0.9	input
DT Yield (13-15 MeV)	$7.67 \pm 0.16 \times 10^{14}$	$1.05 \pm 0.02 \times 10^{15}$	$2.40 \pm 0.05 \times 10^{15}$	3.54×10^{15} (α on) 2.04×10^{15} (no-α)
T_{ion} (keV) [NTOF]	3.02 ± 0.13	3.49 ± 0.13	4.20 ±0.16	2.95
dsr (%)	2.96 ± 0.19%	3.30 ± 0.20	4.21 ± 0.31	3.27
Bangtime (ns) [gamma]	16.76 ± 0.03	16.46 ± 0.05	16.75 ± 0.03	16.62
Burn width (ps) [gamma]	172 ± 40	180 ± 40	156 ± 30	
P0 (μm) [X-ray]	25.6± 4.6	39 ± 1.4	37.4 ± 2.0	34.1
P2/P0 [X-ray]	12.1 ± 9.2 %	-37 ± 7.3%	-24 ± 3.4%	16.7
M0 (um) [X-ray]	33.7 ± 1.7	50.2 ± 1.7	44.7±1.8	-
M4/M0 [X-ray]	58.3 ± 4.7%	7.6 ± 2.4%	3.9±1.7%	-
Velocity (km/s)	296	337	312	312
YOC-1D	60%	35%	70%	-
P (Gbar)	81	53	108	110

Table 1

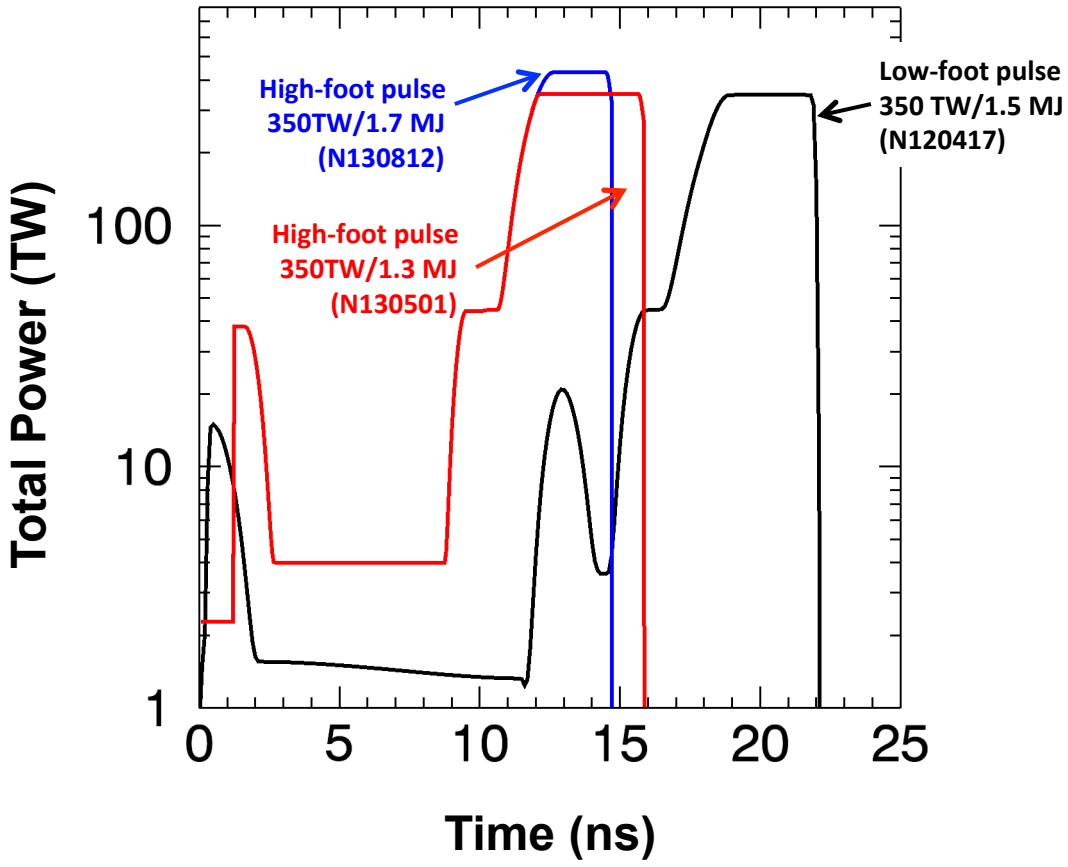
High-foot pulse
350TW/1.7 MJ
(N130812)
High-foot pulse
350TW/1.3 MJ
(N130501)
Low-foot pulse
350 TW/1.5 MJ
(N120417)
Total Power (TW)
100
10
1
0
5
10
15
20
25
Time (ns)

Figure 1

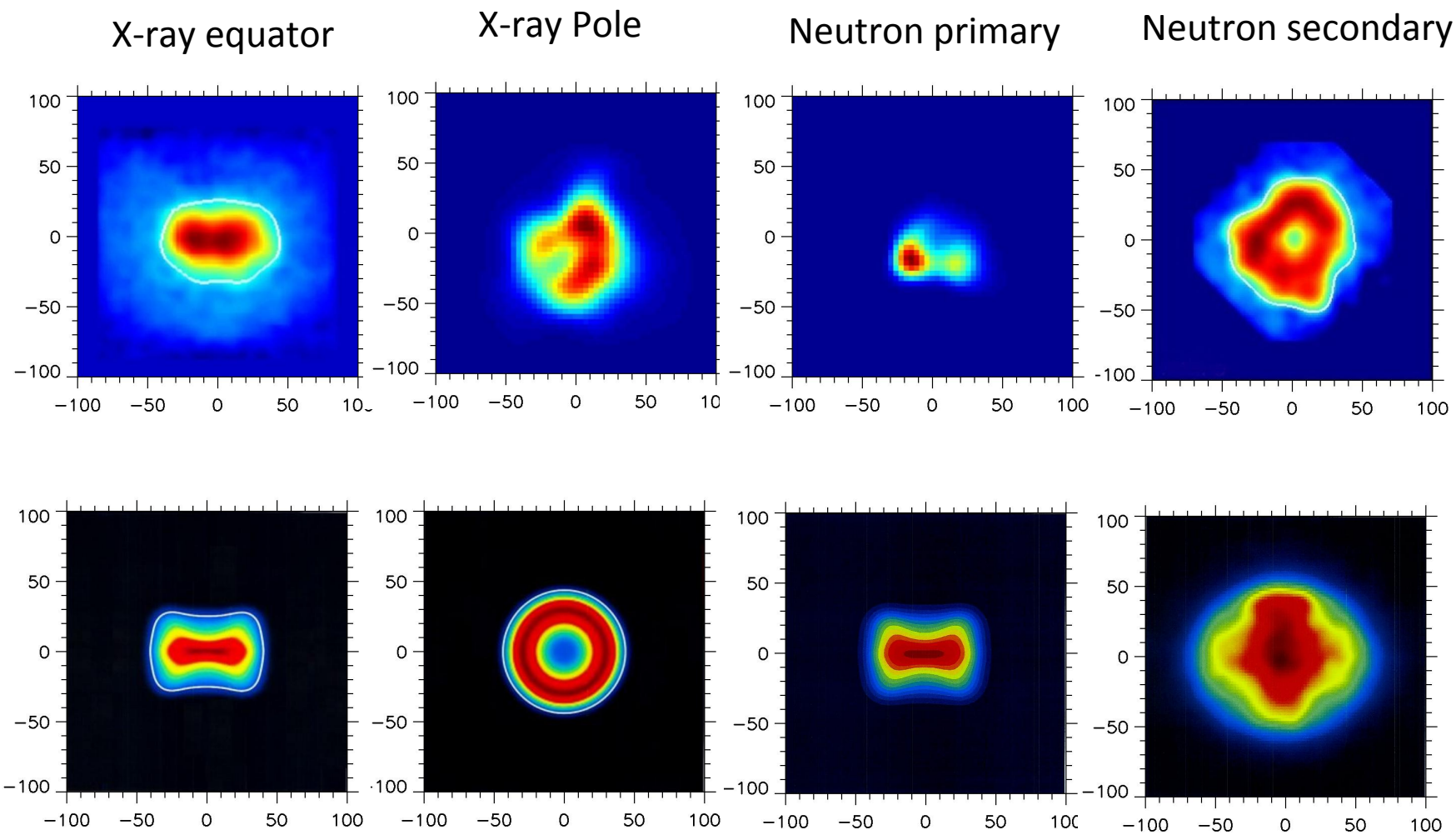

Figure 2

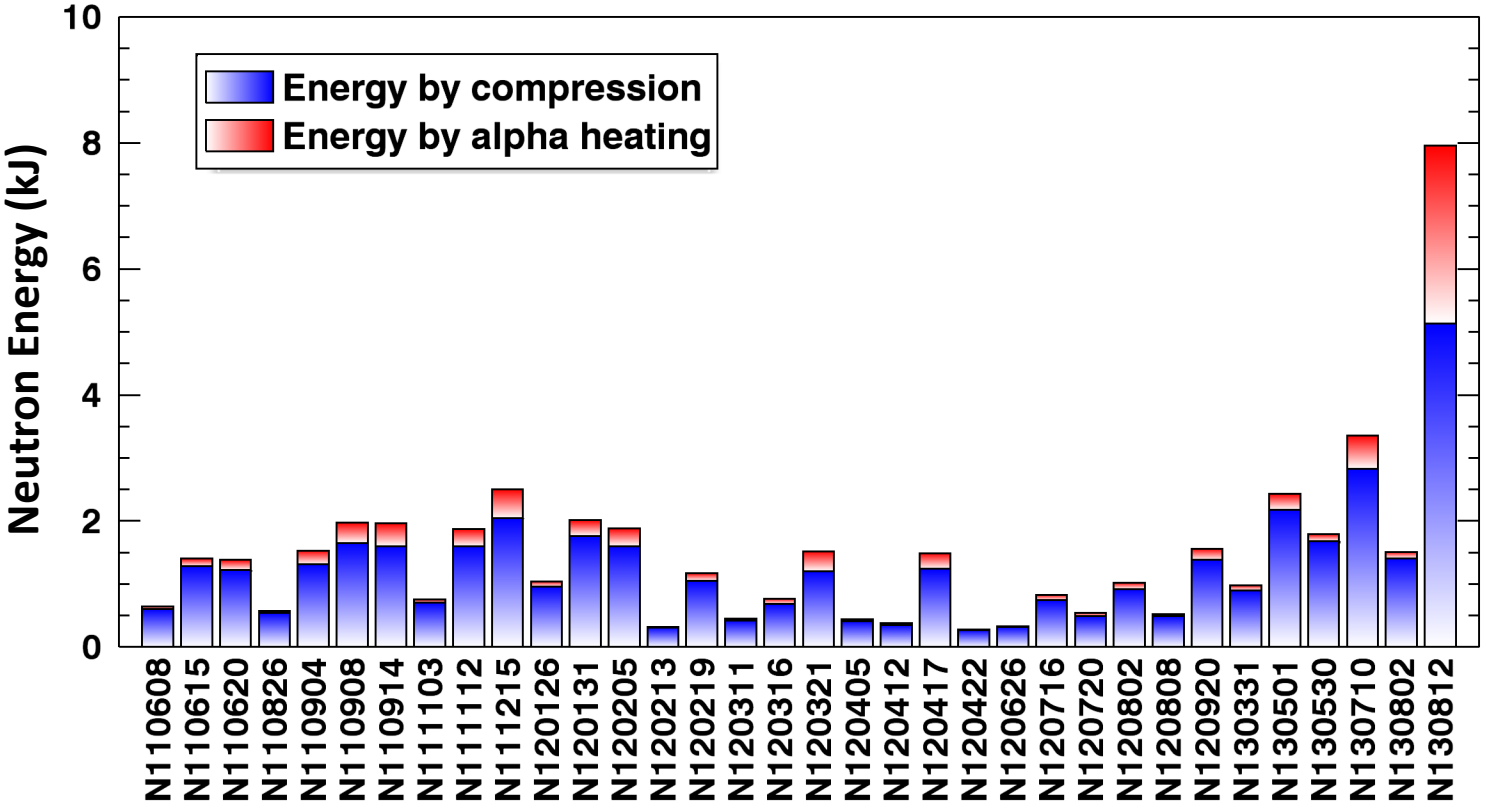
Neutron Energy (kJ)
10
8
6
4
2
0
Energy by compression
Energy by alpha heating
N110608
N110615
N110620
N110826
N110904
N110908
N110914
N111103
N111112
N111215
N120126
N120131
N120205
N120213
N120219
N120311
N120316
N120321
N120405
N120412
N120417
N120422
N120626
N120716
N120720
N120802
N120808
N120920
N130331
N130501
N130530
N130710
N130802
N130812

Figure 3

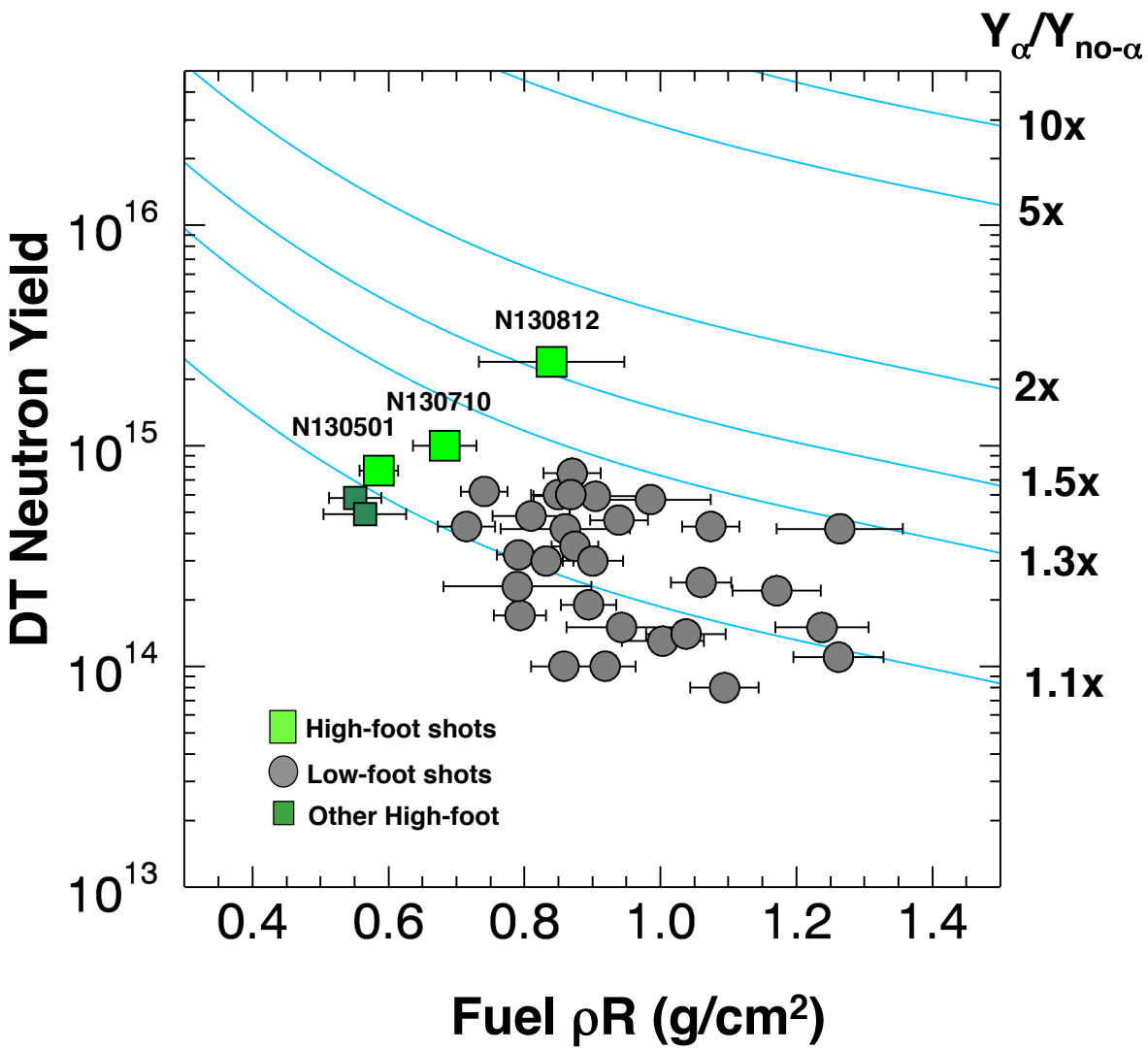
$Y_\alpha/Y_{no\text{-}\alpha}$
10x
5x
2x
1.5x
1.3x
1.1x
DT Neutron Yield
10^{16}
10^{15}
10^{14}
10^{13}
N130812
N130710
N130501
High-foot shots
Low-foot shots
Other High-foot
0.4
0.6
0.8
1.0
1.2
1.4
Fuel ρR (g/cm²)

Figure 4

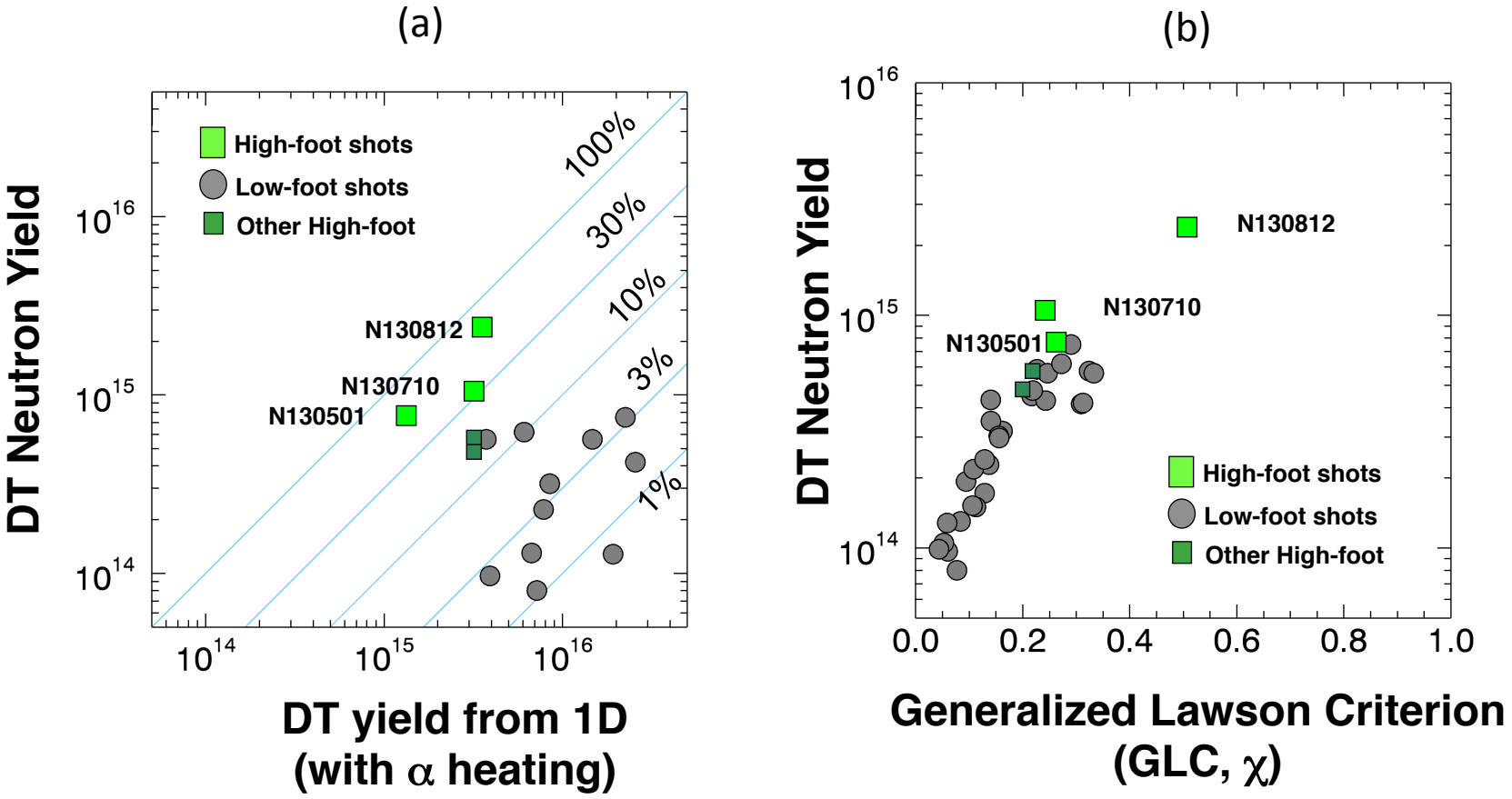
(a)
DT Neutron Yield
10^{16}
10^{15}
10^{14}
High-foot shots
Low-foot shots
Other High-foot
100%
30%
10%
3%
1%
N130812
N130710
N130501
10^{14}
10^{15}
10^{16}
DT yield from 1D
(with α heating)
(b)
DT Neutron Yield
10^{16}
10^{15}
10^{14}
N130812
N130710
N130501
High-foot shots
Low-foot shots
Other High-foot
0.0
0.2
0.4
0.6
0.8
1.0
Generalized Lawson Criterion
(GLC, χ)

Figure 5